

Chapter 6

Model of the Pneumatic Balloon Actuator

6.1 Introduction

This chapter presents a 2D-model of the Pneumatic Balloon Actuator (PBA); it has been established by modeling the physics that seem to underly the behaviour of this actuator. Section 6.2 presents the assumptions and equations on which the model rests and it describes the numerical method developed to solve these equations. Afterwards, Section 6.3 compares the results provided by the numerical model with the experiments performed on two prototypes of PBA. Finally, Section 6.4 discusses and concludes about the developed model.

Remark: The equations of the model have been established by the BEAMS department of the ULB while the solving method of these equations has been developed and implemented in a software by Benjamin Gorissen of the PMA department of the KUL, during its Master's thesis under the supervision of Mich ael De Volder.

6.2 Model

The aim of the model is to predict the evolutions, with respect to the pressure, of the vertical and the horizontal displacements (Δy and Δx respectively in Fig. 6.1) of the free end of a PBA (point *A* in Fig. 6.1).

The assumptions on which the model rests are the following:

1. When pressurized, the PBA deforms in such a way that its cross-section is identical along its width; this cross-section is presented in Fig. 6.1. What happens in the surroundings of the PBA outline is thus assumed to be negligible and this first hypothesis allows an analysis in two dimensions (in the plane xy) of the PBA.
2. The PBA is fixed as a cantilever so that its upper layer is the thinner one of its two layers.
3. The lower layer is modelled as a beam and will hereafter be referred to as "beam".
4. The upper layer is modelled as a membrane and will hereafter be referred to as "membrane".
5. The shear stresses are negligible in the membrane.

6. The normal stresses σ are uniform in the membrane.
7. The membrane thickness e is uniform and remains unchanged when the PBA is pressurized (Poisson's effect is thus assumed to be negligible).
8. The membrane material is homogeneous and follows Hooke's law. The Young's modulus of the membrane E_m is thus assumed to remain unchanged when the membrane deforms.
9. Bernoulli's law is verified for the beam: in the deformed configuration, the straight sections remain plane and perpendicular to the axis of the beam and to all fibres of the beam [39], no warping occurs.
10. The beam material is homogeneous and follows Hooke's law. The Young's modulus of the beam E_b is thus assumed to remain unchanged when the beam deforms.
11. The beam displacements due to shear and normal forces are negligible in comparison to those due to the bending moment.
12. The weights of the beam, the membrane and of the gas inside the PBA are negligible.
13. The pressure p is homogeneous inside the PBA.
14. The beam thickness h (and thus the beam inertia I_b) is uniform and remains unchanged when the PBA is pressurized (Poisson's effect is thus assumed to be negligible).
15. The neutral axis of the beam keeps a constant length L even when the PBA is pressurized.

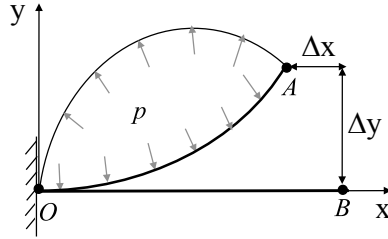


Figure 6.1: Cross-section of a pressurized PBA. The PBA is fixed as a cantilever so that its upper layer is the thinner one of its two layers. The upper layer is modelled as a membrane while the lower one is modelled as a beam. Δy and Δx are the vertical and horizontal displacements of the free end A of the PBA. At rest, OB is the position of the lower layer of the PBA.

Under hypotheses 4 and 5, the behaviour of the membrane is ruled by the Laplace's equation [22]:

$$\gamma \left(\frac{1}{r_1} + \frac{1}{r_2} \right) = p_{in} - p_{out} \quad (6.1)$$

where γ is the surface tension in the membrane, r_1 and r_2 are the principal curvature radii of the membrane and $p_{in} - p_{out}$ is the pressure difference between the inside and the outside of the membrane. p_{out} will here assumed to be zero and the pressure inside the membrane will be noted as p . Due to hypothesis 1, one curvature of the membrane is zero and (6.1) becomes

$$\frac{\gamma}{r} = p, \quad (6.2)$$

where r is the radius of curvature of the membrane. Due to hypothesis 6, the surface tension is uniform in the membrane. As a consequence, r is constant along the membrane which thus takes the shape of an arc of circle.

Under hypotheses 3, 9, 10 and 11, the deformation of the beam is ruled by the Euler-Bernoulli's equation [39]:

$$\frac{1}{R(s)} = \frac{M(s)}{E_b I_b}, \quad (6.3)$$

where R is the curvature radius of the beam, M is the bending moment due to the loads applied to the beam and $I_b = \frac{bh^3}{12}$, with b the width of the PBA (along axis z). As shown in Fig. 6.2, the beam is subjected to a concentrated load \bar{F} applied by the pressurized membrane and to pressure p (i.e. a distributed load), or more precisely to $q = pb$. P is the

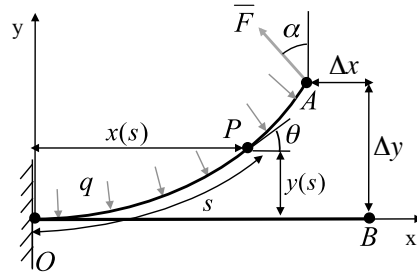


Figure 6.2: Loads applied to the PBA lower layer, which is modelled as a beam. The beam is subjected to a concentrated load \bar{F} applied by the pressurized membrane and to pressure p (i.e. a distributed load), or more precisely to $q = pb$. P is the point of the beam where bending moment $M(s)$ is evaluated. Its coordinates are $x(s)$ and $y(s)$. s is the distance along the beam between points O and P . θ is the angle between the horizontal direction and the tangential direction of the beam at point P . α is the angle of inclination of force \bar{F} , with reference to the vertical direction. Δy and Δx are the vertical and horizontal displacements of the free end A of the PBA. When the PBA is not pressurized, OB is the position of the beam.

point of the beam where bending moment $M(s)$ is evaluated. Its coordinates are $x(s)$ and $y(s)$. s is the distance along the beam between points O and P and θ is the angle between the horizontal direction and the tangential direction of the beam at point P . Since

$$\frac{1}{R(s)} = \frac{d\theta(s)}{ds} \quad [39], \quad (6.4)$$

(6.3) becomes:

$$\frac{d\theta(s)}{ds} = \frac{M(s)}{E_b I_b}. \quad (6.5)$$

Solving (6.5) gives a function $\theta = \theta(s)$ from which the coordinates of the points of the deformed beam can be computed using the following expressions:

$$x(s) = \int_0^s \cos(\theta(u)) du \quad (6.6)$$

$$y(s) = \int_0^s \sin(\theta(u)) du. \quad (6.7)$$

The X- and Y-displacements of the PBA free end are given by

$$\Delta x = L - x(L) \quad (6.8)$$

and

$$\Delta y = y(L) \quad (6.9)$$

and the coordinates of end point A are given by

$$x_A = x(L) \quad (6.10)$$

and

$$y_A = y(L). \quad (6.11)$$

For the configuration presented in Fig. 6.2, the expression of bending moment $M(s)$ is:

$$\begin{aligned} M(s) = F & [\cos(\alpha)(L - \Delta x - x(s)) + \sin(\alpha)(\Delta y - y(s))] \\ & - \int_s^L q \cos(\theta(u))(x(u) - x(s))du \\ & - \int_s^L q \sin(\theta(u))(y(u) - y(s))du, \end{aligned} \quad (6.12)$$

where F is the norm of force \bar{F} and α is the angle of inclination of force \bar{F} , with reference to the vertical direction (see Fig. 6.2). To get rid of the integrals, an equation based on the shearing force dM/ds instead of the bending moment M can be used [24]. To obtain this equation, (6.5) is differentiated with respect to s and, with assumptions 10 and 14, this gives:

$$\frac{d^2\theta(s)}{ds^2} = \frac{1}{E_b I_b} \frac{dM(s)}{ds}. \quad (6.13)$$

To compute the expression of dM/ds , the following formula is used

$$\begin{aligned} \frac{d}{ds} \int_{w(s)}^{v(s)} f(s, u) du &= \frac{dv(s)}{ds} f(s, v(s)) - \frac{dw(s)}{ds} f(s, w(s)) \\ &+ \int_{w(s)}^{v(s)} \frac{\partial f(s, u)}{\partial s} du, \end{aligned} \quad (6.14)$$

and it leads to:

$$\begin{aligned} \frac{dM(s)}{ds} &= -F [\cos(\alpha) \cos(\theta(s)) + \sin(\alpha) \sin(\theta(s))] \\ &+ q [\cos(\theta(s))(L - \Delta x - x(s)) + \sin(\theta(s))(\Delta y - y(s))]. \end{aligned} \quad (6.15)$$

Equation (6.13) becomes then:

$$\begin{aligned} \frac{d^2\theta(s)}{ds^2} &= \frac{-F}{E_b I_b} [\cos(\alpha) \cos(\theta(s)) + \sin(\alpha) \sin(\theta(s))] \\ &+ \frac{q}{E_b I_b} [\cos(\theta(s))(L - \Delta x - x(s)) + \sin(\theta(s))(\Delta y - y(s))], \end{aligned} \quad (6.16)$$

with the boundary conditions

$$\theta|_{s=0} = 0 \quad (6.17)$$

and

$$\frac{d\theta}{ds}|_{s=L} = 0. \quad (6.18)$$

Equation (6.16) can be used to compute the X- and Y-displacements Δx and Δy but firstly F and α need to be evaluated. The following equations allow to determine F and α since p is given and since the coordinates (x_A, y_A) of end point A are assumed:

$$\|\overline{OA}\| = \sqrt{(x_A)^2 + (y_A)^2} \quad (6.19)$$

$$\tan(\epsilon) = \frac{y_A}{x_A} \quad (6.20)$$

$$2\beta r = L + \Delta L \quad (6.21)$$

$$\sigma = E_m \frac{\Delta L}{L} \quad (6.22)$$

$$\frac{\gamma}{r} = p \quad (6.23)$$

$$r = \frac{\|\overline{OA}\|}{2 \sin(\beta)} \quad (6.24)$$

$$\gamma = \sigma e \quad (6.25)$$

$$F = \gamma b \quad (6.26)$$

$$\alpha = \frac{\pi}{2} - \beta + \epsilon \quad (6.27)$$

where ΔL and $\frac{\Delta L}{L}$ are the lengthening and the strain of the deformed membrane, respectively. Angles ϵ and β are defined as shown in Fig. 6.3.

Equations (6.19), (6.20), (6.21), (6.24) and (6.27) are geometrically deduced from Fig. 6.3. Equation (6.22) is the relation between the stress σ and the strain $\frac{\Delta L}{L}$ of the membrane. Equation (6.23) is the Laplace's equation (6.2). Equation (6.25) is the relation between the surface tension γ and the stress σ of the membrane. Equation (6.26) is the relation between the surface tension γ of the membrane and the norm F of the force \overline{F} developed by the pressurized membrane.

Remark: As can be seen from the previous equations, the model is suitable for compressible as well as for incompressible fluids.

Equation (6.16) has the following shape:

$$\frac{d^2\theta(s)}{ds^2} = f(\theta(s)) \quad (6.28)$$

and it can be approximated by the following expression:

$$\frac{\theta_{i+1} - 2\theta_i + \theta_{i-1}}{(\Delta s)^2} = f(\theta_i), \quad (6.29)$$

with $\theta_i = \theta(s)|_{s=i\Delta s}$, $i = 0, \dots, N$ and $\Delta s = \frac{L}{N}$ (see Fig. 6.4).

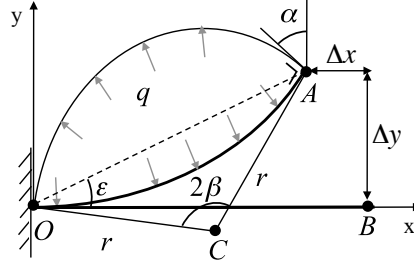


Figure 6.3: Cross-section of a pressurized PBA. The PBA upper layer is modelled as a membrane while the lower one is modelled as a beam. The beam is subjected to a concentrated load \bar{F} applied by the pressurized membrane and to pressure p (i.e. a distributed load), or more precisely to $q = pb$. α is the angle of inclination of force \bar{F} , with reference to the vertical direction. C and r are the curvature centre and radius of the deformed membrane, respectively. Angles ϵ and β are defined as shown in the figure. Δy and Δx are the vertical and horizontal displacements of the free end A of the PBA. When the PBA is not pressurized, OB is the position of the beam.

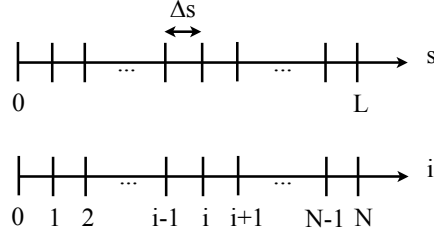


Figure 6.4: s is the distance along the beam. s ranges from 0 to L . The length L of the PBA is divided into segments of length Δs . The parameter i is used in the approximation of the equation $\frac{d^2\theta}{ds^2} = f(\theta(s))$. The length along the beam corresponding to i is $s = i\Delta s$.

The two following equations are the boundary conditions of equation (6.29); they correspond to the boundary conditions (6.17) and (6.18), respectively:

$$\theta_0 = 0 \quad (6.30)$$

and

$$\theta_{N-1} = \theta_N \quad (6.31)$$

Equation (6.29) is then used iteratively to compute the solution θ_i with $i = 0, \dots, N$; this is done as follows:

$$\frac{\theta_{i+1}^{n+1} - 2\theta_i^{n+1} + \theta_{i-1}^{n+1}}{(\Delta s)^2} = f(\theta_i^n) \quad (6.32)$$

1. The initial solution $n = 0$ ($\theta_i^{n=0}$ with $i = 0, \dots, N$) is used to compute $f(\theta_i^n)$ (including the calculations of F and α) and equation (6.32) allows then to compute the solution $n = 1$ ($\theta_i^{n=1}$ with $i = 0, \dots, N$).
2. If the solutions $n = 1$ and $n = 0$ are too far from each other, the solution $n = 1$ ($\theta_i^{n=1}$ with $i = 0, \dots, N$) is used to compute $f(\theta_i^n)$ and equation (6.32) allows then to compute the solution $n = 2$ ($\theta_i^{n=2}$ with $i = 0, \dots, N$).
3. If the solutions $n = 2$ and $n = 1$ are too far from each other, etc.

The iterations are repeated until the method converges to a solution $n = j$ ($\theta_i^{n=j}$ with $i = 0, \dots, N$); this solution is such that the solutions $n = j$ and $n = j - 1$ are close enough to each other, i.e.:

$$\frac{\sum_{i=0}^N (\theta_i^j - \theta_i^{j-1})^2}{\sum_{i=0}^N (\theta_i^j)^2} < 1\% \quad (6.33)$$

A database comprising hundred initial solutions has been established. These initial solutions are beams whose free end has displaced upwards or downwards. For a given initial solution, if after fifty iterations the method has not converged, the next initial solution of the database is tried.

The model and its solving method have been implemented in a software. The characteristics of the PBA (L, b, e, h, E_m and E_b) and the pressure p have to be provided to the software which computes the corresponding deformed configuration of the PBA and in particular the displacements Δx and Δy of the PBA free end (see Fig. 6.5).

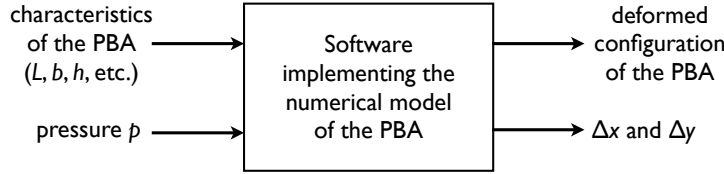


Figure 6.5: Inputs and outputs of the software implementing the numerical model of the PBA.

In practice, when performing experiments with the test bench as described in Chapter 5, it is not the pressure p that is imposed but the displacement u of the cylinder piston (see Fig. 6.6). It could then be interesting to establish the relationship existing between p and u . This relationship could then be added to the software so that its inputs would be the characteristics of the PBA and u , rather than p (see Fig. 6.7).

For a given pressure p , the software provides the complete deformed configuration of the PBA. The inner volume V_{PBA} of the PBA can be computed from this deformed configuration and assuming $V_{PBA} = 0$ when $u = 0$, V_{PBA} can be related to u as follows:

- in the case of an incompressible fluid: the total volume of fluid V equals Sd (S is the cross-section of the cylinder and d is its length (see Fig. 6.6)) and

$$V_{PBA} = Su \quad (6.34)$$

- in the case of a compressible fluid: the total volume V_{atm} at the atmospheric pressure p_{atm} equals Sd . The temperature is assumed to be constant and since the fluidic circuit is closed, the quantity of fluid is also constant. After a piston displacement u , the PBA has a volume V_{PBA} and the total volume is $V_1 = V_{PBA} + S(d - u)$ at the absolute pressure $p_1 = p_{atm} + p$. The gas law leads thus to:

$$p_{atm}V_{atm} = p_1V_1 \quad (6.35)$$

and more precisely to

$$p_{atm}Sd = (p_{atm} + p)(V_{PBA} + S(d - u)) \quad (6.36)$$

Establishing the relationship between u and p for a given PBA can thus be done as follows:

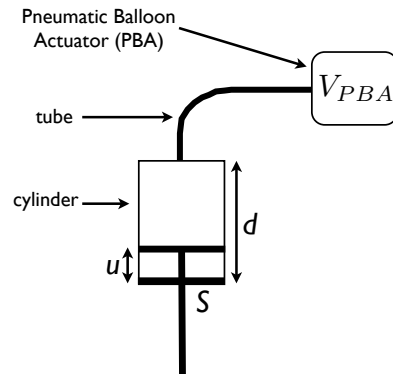


Figure 6.6: PBA connected to a cylinder with a tube. When the cylinder piston performs a displacement u , the PBA inflates and its volume is V_{PBA} . When $u = 0$, it is assumed that $V_{PBA} = 0$. S is the cross-section of the cylinder.

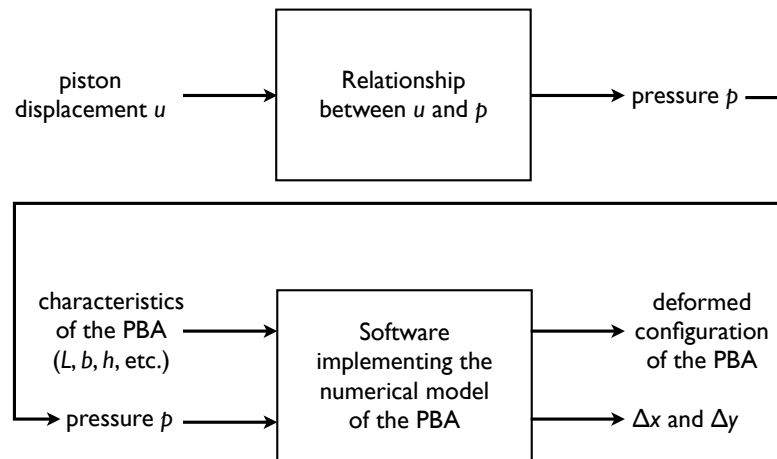


Figure 6.7: The relationship existing between the piston displacement u and the pressure p can be added to software implementing the numerical model of the PBA. Hence, the inputs of the software would be the characteristics of the PBA and u , rather than p .

1. For different pressures p^* , the deformed configuration of the PBA is calculated with the software and the corresponding inner volume V_{PBA}^* of the PBA is computed from this deformed configuration.
2. Equation (6.34) or (6.36) is then used to calculate the piston displacements u^* corresponding to the different PBA volumes V_{PBA}^* .
3. The pressure values p^* are plotted with respect to the corresponding piston displacements u^* ; this graph represents the relationship existing between u and p for the studied PBA.

6.3 Results of the model

6.3.1 Modeling of the original PBA

The original PBA described in [49] has been modeled with the numerical model described in the previous section. The original PBA will hereafter be referred to as "Konishi's PBA" to distinguish it from its modeled counterpart.

The size of Konishi's PBA is 16 mm × 16 mm while the size of its cavity is 10 mm × 10 mm; the cavity is located at the centre of the actuator. Only this cavity can be modeled by the numerical model and the parameters of Konishi's PBA are summarized in Table 6.1. The values of the Young's moduli of the silicone rubber and the polyimide, given in Table 6.1, have been looked for with the Cambridge Engineering Selector (CES) software. Indeed, these values were not specified in the description of Konishi's PBA in [49].

Parameter	Value
length of the cavity L	10 10^{-3} m
width of the cavity b	10 10^{-3} m
length of the actuator L'	16 10^{-3} m
width of the actuator b'	16 10^{-3} m
membrane thickness e	200 10^{-6} m
beam thickness h	50 10^{-6} m
membrane Young's modulus E_m	silicone rubber: 0.005 to 0.05 10^9 Pa
beam Young's modulus E_b	polyimide: 2.07 to 2.76 10^9 Pa
pressure p	$p_{max} = 65.1$ kPa
beam inertia I_b	$I_b = \frac{b'h^3}{12} + 2\frac{E_m}{E_b} \left[\frac{\frac{b'-b}{2}e^3}{12} + e\frac{b'-b}{2}\left(\frac{e+h}{2}\right)^2 \right]$

Table 6.1: Parameters of Konishi's PBA described in [49].

The total width b' of Konishi's PBA is 16 mm while the width b of the cavity equals 10 mm and the surrounding edges of the cavity, where the membrane and the beam are glued to each other, contribute to the inertia of the beam. Fig. 6.8 presents the cross-section of the actuator; the areas contributing to the inertia of the beam are colored in grey. As can be seen a part of the membrane (areas no. 1 and 2) contributes to it. To take the contributions of areas no. 1, 2 and 3 into account, the inertia of the beam is computed as follows:

$$I_b = \frac{b'h^3}{12} + 2\frac{E_m}{E_b} \left[\frac{\frac{b'-b}{2}e^3}{12} + e\frac{b'-b}{2}\left(\frac{e+h}{2}\right)^2 \right] \quad (6.37)$$

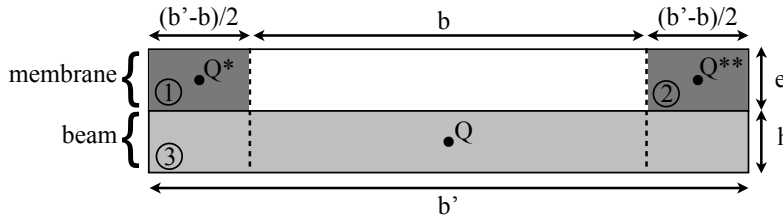


Figure 6.8: Cross-section of Konishi's PBA described in [49]. The grey area contributes to the inertia of the beam.

Fig. 6.10, 6.12 and 6.13 present the results provided by the numerical model for $p = 2$ kPa, $E_m = 0.0275 \cdot 10^9$ Pa and $E_b = 2.415 \cdot 10^9$ Pa (the values chosen for E_m and E_b are the mid

values of the ranges given in Table 6.1):

- As can be seen in Fig. 6.10, when the pressure increases up to 0.76 kPa, the free end of the modeled PBA moves upwards; this behaviour corresponds to that of Konishi's PBA and is thus physically correct. Above 0.76 kPa, the free end of the modeled PBA moves downwards. Hence, according to the numerical model, the PBA presents a bidirectional motion: when pressurized, the PBA moves its end upwards, until a given pressure level is reached and above this level, the PBA tip is moved downwards. This behaviour has been experimentally noticed by [50] and by Benjamin Gorissen and Michael De Volder of the KUL, for PBAs made of two layers of the same material (the same PDMS) and of different thicknesses (see Fig. 6.11). However, Konishi's PBA is made of two different materials and no bidirectional motion has been reported for it in [49]. As can be noticed in Fig. 6.12 and 6.13, the numerical model predicts that the change in actuation direction happens instantaneously for a given pressure level. However, in practice, this happens continuously. As can be seen in Fig. 6.10, the representation of the membrane is not correct when the PBA tip moves downwards.

- As can be seen in Fig. 6.12, for the upwards motion phase, the Y-displacements Δy_0 predicted by the numerical model:
 - are of the same order of magnitude than those measured on Konishi's PBA. The numerical model predicts the tip displacements of the PBA cavity, as presented in Fig. 6.1. However, the measurements performed on Konishi's PBA are the tip displacements of the 16 mm \times 16 mm actuator and not the tip displacements of its 10 mm \times 10 mm cavity (see Fig. 6.9). The tip displacements measured on Konishi's PBA are thus larger than the tip displacements of its cavity.

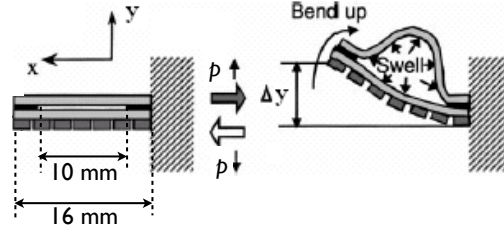


Figure 6.9: Schematic cross-section views of Konishi's PBA (described in [49]): PBA at rest and pressurized PBA (p = pressure) on the left hand side and the right hand side, respectively. The PBA is fixed as a cantilever and the displacements are measured at its tip. Figure adapted from [49].

- have an evolution with the pressure p similar to that of the measurements performed on Konishi's PBA. However, the maximum pressure $p^* = 0.76$ kPa, for which upwards displacements are predicted by the numerical model, is nearly ninety times smaller than for Konishi's PBA ($p^* = 65.1$ kPa).

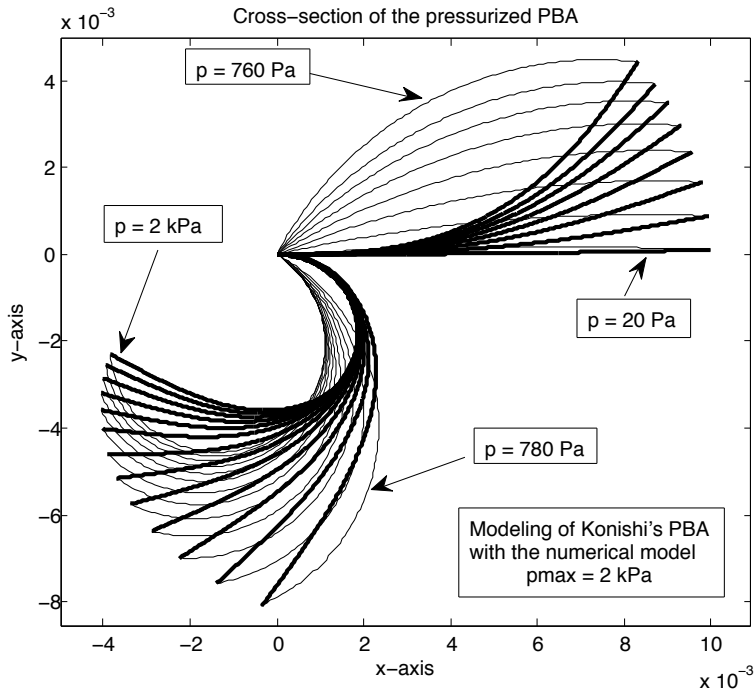


Figure 6.10: Modeling of Konishi's PBA (described in [49]) with the numerical model: cross-section of the PBA for a pressure p up to 2 kPa (the different representations of the cross-section correspond to pressures spaced out by about 100 Pa). The thin and thick lines represent the membrane and the beam, respectively. As can be seen, the numerical model predicts a bidirectional motion of the PBA.

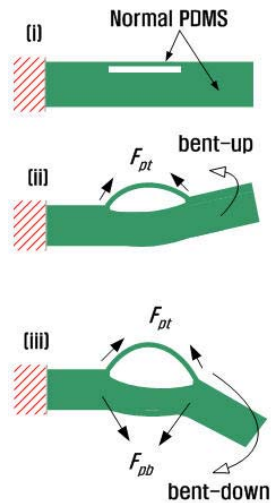


Figure 6.11: Bidirectional motion of a PBA made of two layers of the same material (the same PDMS) and of different thicknesses (see (i) for the PBA at rest). When pressurized, the PBA moves its end upwards (see (ii)) until a given pressure level is reached; above this level, the PBA tip is moved downwards (see (iii)). Figure from [50].

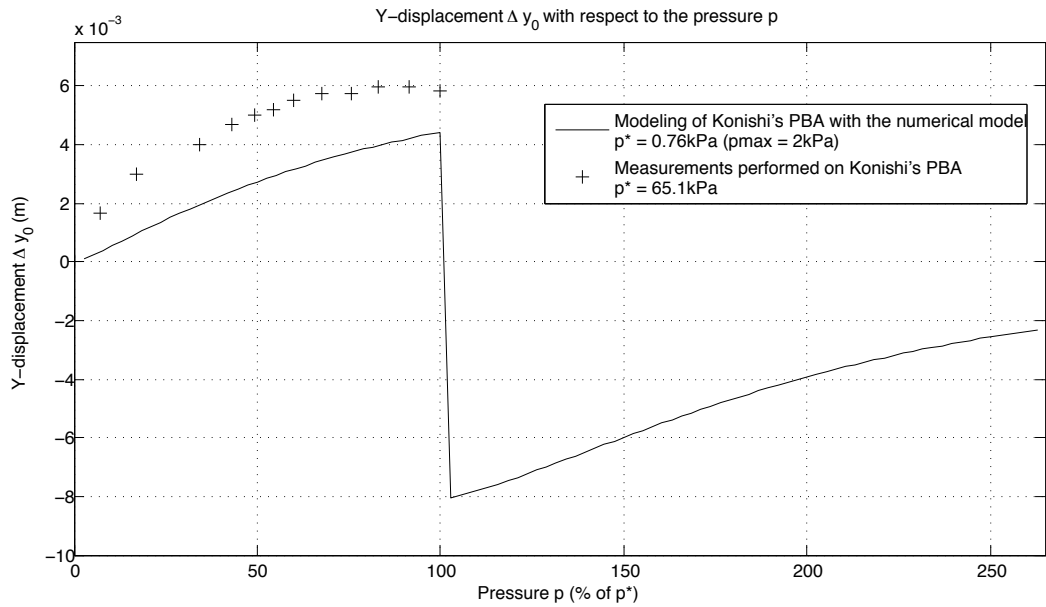


Figure 6.12: Y-displacement Δy_0 of the PBA free end with respect to the pressure p . Comparison between the measurements performed on Konishi's PBA (described in [49]) and the results provided by the numerical model. The measurements on Konishi's PBA come from [49]. As can be seen, the numerical model predicts a bidirectional motion of the PBA and in the upwards motion phase, the measurements are of the same order of magnitude than the results of the numerical model.

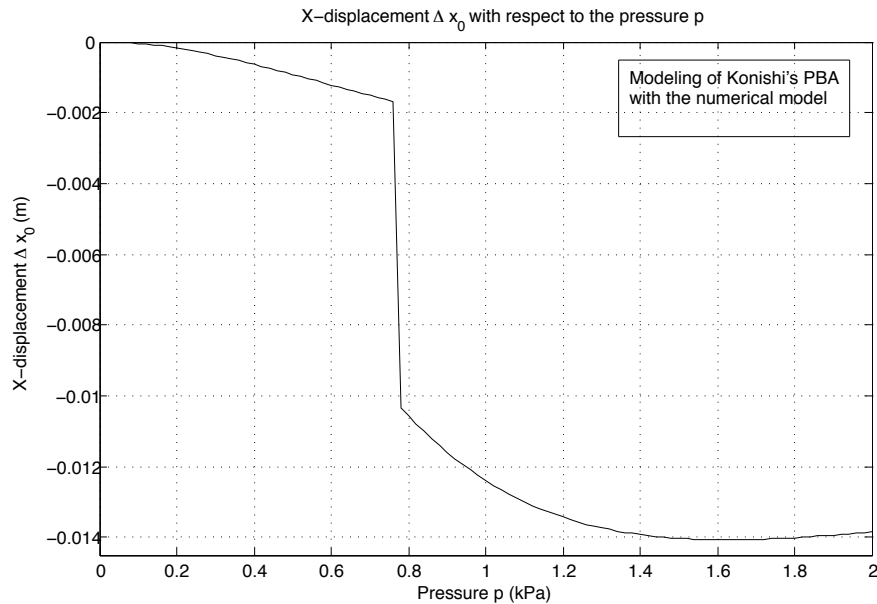


Figure 6.13: Modeling of Konishi's PBA (described in [49]) with the numerical model: X-displacement Δx_0 of the PBA free end with respect to the pressure p . As can be seen, the numerical model predicts a bidirectional motion of the PBA.

6.3.2 Modeling of the test bench PBA

The PBA used on the test bench and described in Section 4.2.2 has been modeled with the numerical model. This prototype will hereafter be referred to as "test bench PBA" to distinguish it from its modeled counterpart.

The size of the test bench PBA is 50 mm × 60 mm while the size of its cavity is 40 mm × 40 mm. Only this cavity can be modeled by the numerical model and the parameters of the test bench PBA are summarized in Table 6.2. The values of the polyurethane Young's modulus, given in Table 6.2, have been looked for with the Cambridge Engineering Selector (CES) software. Indeed, the PRONAL company which has manufactured the actuators could not specify these values.

Parameter	Value
length of the cavity L	40 10^{-3} m
width of the cavity b	40 10^{-3} m
length of the actuator L'	50 10^{-3} m
width of the actuator b'	60 10^{-3} m
membrane thickness e	0.5 10^{-3} m
beam thickness h	1 10^{-3} m
membrane and beam Young's moduli E_m and E_b	polyurethane: minimum found value = 0.0025 10^9 Pa maximum found value = 2.07 10^9 Pa
pressure p	max 20 – 30 kPa (see Section 4.2.2)
beam inertia I_b	$I_b = \frac{b'h^3}{12} + 2\frac{E_m}{E_b} \left[\frac{b'-b}{12}e^3 + e\frac{b'-b}{2}\left(\frac{e+h}{2}\right)^2 \right]$

Table 6.2: Parameters of the test bench PBA.

The total width b' of the test bench PBA is 60 mm while the width b of the cavity equals 40 mm and the surrounding edges of the cavity, where the membrane and the beam are fixed to each other, contribute to the inertia of the beam. Hence, exactly as for Konishi's PBA, Fig. 6.8 presents the cross-section of the actuator and the areas contributing to the inertia of the beam are colored in grey. To take the contributions of areas no. 1, 2 and 3 into account, the inertia of the beam is computed with the formula (6.37).

Fig. 6.15 to 6.18 present the results provided by the numerical model for $p = 25$ kPa and $E_m = E_b = 1.03625 \cdot 10^9$ Pa (the value chosen for E_m and E_b is the mid value of the range given in Table 6.2):

- As can be seen in Fig. 6.15, when the pressure p increases up to 25 kPa, the free end of the modeled PBA moves upwards. This behaviour corresponds to that of the test bench PBA and is thus physically correct.
- As can be seen in Fig. 6.16, 6.17 and 6.18, when the pressure p increases, the PBA free end moves upwards and Δx_0 and Δy_0 increase in absolute value. Besides, it can be noticed that:
 - the displacements Δx_0 and Δy_0 predicted by the numerical model are of the same order of magnitude than those measured on the test bench PBA.
 - the displacements Δy_0 predicted by the numerical model are larger than those measured on the test bench PBA, all the more that the numerical model predicts the displacements of the cavity tip (see point A' in Fig. 6.14) and that, as explained in Section 4.3, the measurements Δx_0 and Δy_0 made on the test bench PBA are the displacements of a point located 5 mm far from the cavity tip (see point B' in Fig. 6.14). This implies than the tip displacements measured on the test bench PBA are larger, in absolute value, than the tip displacements of its cavity.

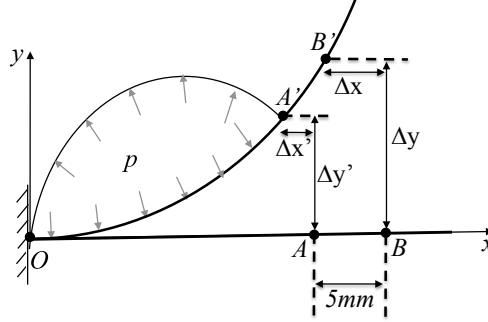


Figure 6.14: Schematic cross-section of the test bench PBA. The numerical model predicts the X- and Y- displacements of point A' ($\Delta x'_0$ and $\Delta y'_0$) while the measurements performed on the test bench PBA are the X- and Y- displacements of point B' (Δx_0 and Δy_0).

- the displacements Δx_0 of the cavity tip predicted by the numerical model are smaller, in absolute value, than the measurements performed on the test bench PBA but, as explained before, these measurements are larger, in absolute value, than the tip displacements of the cavity (see Fig. 6.14).
- the displacements Δy_0 predicted by the numerical model present an evolution with the pressure p similar to that of the measurements performed on the test bench PBA. This is not the case for the displacements Δx_0 predicted by the numerical model.

As already said, the displacements Δy_0 predicted by the numerical model are larger than those measured on the test bench PBA for the same pressure. The predictions of the numerical model have been achieved for large Young's moduli E_m and E_b . If the Young's moduli and the pressure keep the same ratio, the same displacements Δx_0 and Δy_0 are predicted by the model. This means that if the Young's moduli of the test bench PBA are in reality ten times smaller than those used to establish the curves of Fig. 6.15 to 6.18, the same displacements Δx_0 and Δy_0 will be predicted by the numerical model but for a maximum pressure that is ten times smaller than $p = 25$ kPa. However, since the actual Young's moduli are not known, it is difficult to conclude about the results provided by the numerical model.

If the pressure is increased above 25 kPa, the numerical model predicts that the test bench PBA has a bidirectional motion and that the change in actuation direction happens for $p = 32$ kPa.

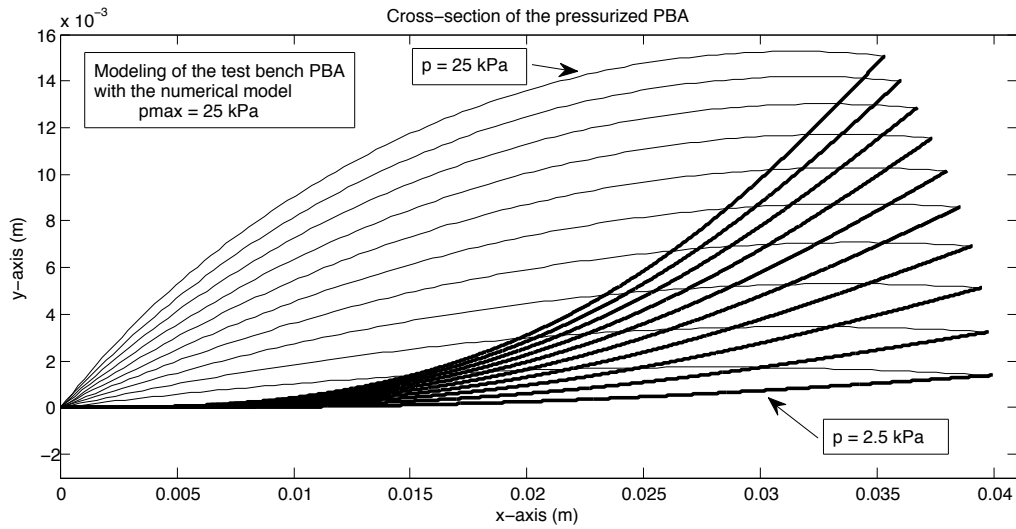


Figure 6.15: Modeling of the test bench PBA with the numerical model: evolution of the PBA cross-section with the pressure p . When the pressure p increases, the PBA free end moves upwards. The thin and thick lines represent the membrane and the beam, respectively. The different representations of the cross-section correspond to pressures spaced out by 2.5 kPa.

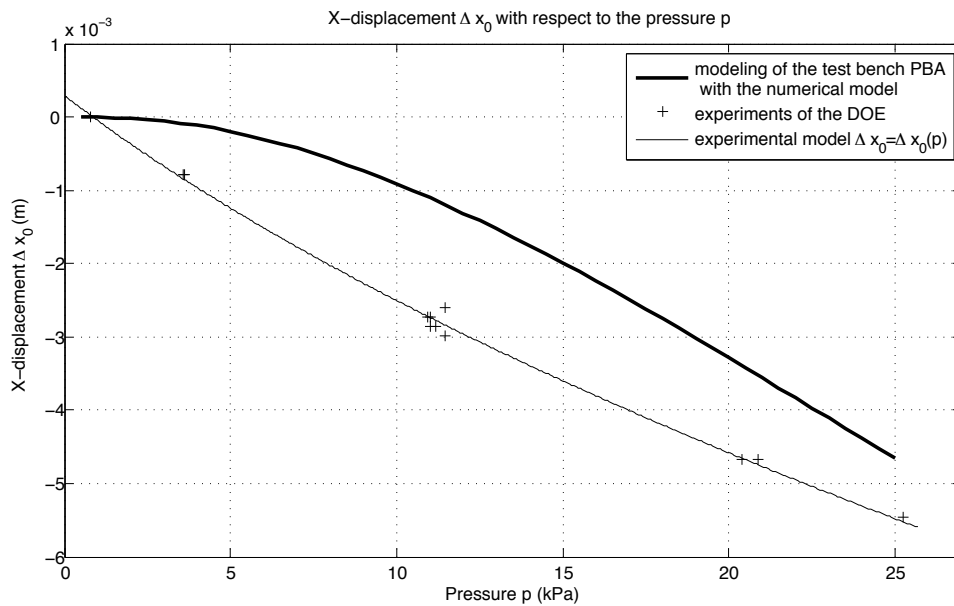


Figure 6.16: X-displacement Δx_0 of the PBA free end with respect to the pressure p . When the pressure p increases, the PBA free end moves upwards and Δx_0 increases in absolute value. The thick line is computed by the numerical model. The crosses are the experiments of the DOE (described in Section 5.2.1) that has been applied to the test bench PBA; the thin line is the experimental model $\Delta x_0 = \Delta x_0(p)$ deduced from these experiments.

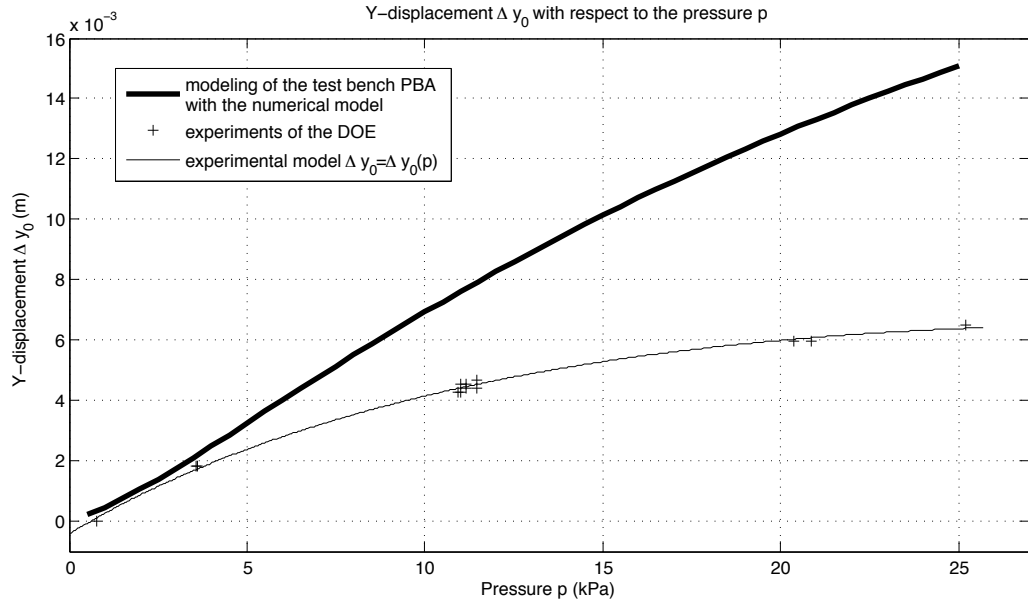


Figure 6.17: Y-displacement Δy_0 of the PBA free end with respect to the pressure p . When the pressure p increases, the PBA free end moves upwards and Δy_0 increases. The thick line is computed by the numerical model. The crosses are the experiments of the DOE (described in Section 5.2.1) that has been applied to the test bench PBA; the thin line is the experimental model $\Delta y_0 = \Delta y_0(p)$ deduced from these experiments.

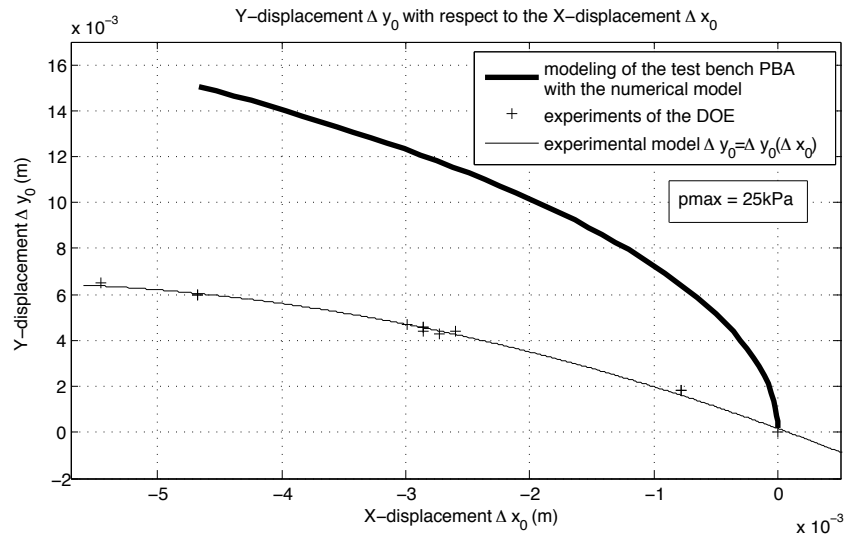


Figure 6.18: Y-displacement Δy_0 of the PBA free end with respect to its X-displacement Δx_0 . When the pressure p increases, the PBA free end moves upwards and Δx_0 and Δy_0 increase in absolute value. The thick line is computed by the numerical model. The crosses are the experiments of the DOE (described in Section 5.2.1) that has been applied to the test bench PBA; the thin line is the experimental model $\Delta y_0 = \Delta y_0(\Delta x_0)$ deduced from these experiments.

6.4 Discussion and conclusions

As already said,

- the upwards Y-displacements Δy_0 predicted by the numerical model are of the same order of magnitude than the measurements made on Konishi's PBA but they are achieved for a pressure that is much lower than the actual pressure.
- the Y-displacements Δy_0 predicted by the numerical model are larger than those measured on the test bench PBA for the same pressure. Besides, these predictions have been achieved for Young's moduli E_m and E_b that are maybe too large compared to the actual Young's moduli of the test bench PBA.

This means that the PBA of the numerical model is less stiff than its real counterpart. This can be explained by the fact that some of the assumptions on which the model rests are too far from the reality.

Indeed, according to hypothesis 1: "*When pressurized, the PBA deforms in such a way that its cross-section is identical along its width; this cross-section is presented in Fig. 6.1. What happens in the surroundings of the PBA outline is thus assumed to be negligible and this first hypothesis allows an analysis in two dimensions (in the plane xy) of the PBA*".

Hence, the model assumes that the membrane is fixed to the beam only by the two sides placed in the width direction. In practice however, both layers of the PBA are fixed to one another along their four sides. The model neglects thus the forces applied to the membrane along the sides placed in the length direction and the cross-section of the PBA is not identical along the width. Hence, in practice, the shear stresses are probably not negligible in the membrane (assumption 5) and the stresses σ not uniform in the membrane (assumption 6). By neglecting all these phenomena, the model leads to a PBA less rigid than the real prototype.

Besides, in the case of Konishi's PBA and of the test bench PBA, hypothesis 3 is not valid. Indeed, according to this assumption, the lower PBA layer is modeled as a beam. However, Konishi's PBA and the test bench PBA have dimensions such that $L = b$ while by definition, a beam has a length which is larger than its two other dimensions. Hence, the bottom layer of Konishi's PBA and of the test bench PBA should better be modeled by a plate.

In addition to this, in the case of Konishi's PBA, since the cavity is placed at the centre of the actuator, the membrane applies a pulling force F at two places to the beam: at its beginning and at its end. However, the numerical model only takes into account the pulling force applied to the end of the beam.

In conclusion, a PBA modeled with the numerical model will be less stiff than its real counterpart and some of the assumptions on which the model rests are not verified in reality; this leads to large differences between the predictions provided by the model and the measurements performed on the prototypes (e.g. too large displacements, too low pressures, incorrect shape of the evolution of the X-displacements Δx_0 with respect to the pressure). However, the numerical model is able to predict the bidirectional behaviour of a PBA and allows to better understand the physics underlying. The bidirectional behaviour is due to the pressure applied to the beam and to the force applied by the pressurized membrane to the beam. If the force applied by the membrane is predominant, the PBA free end moves upwards while if the pressure is predominant, it moves downwards.

It has to be mentioned that the numerical model seems to predict that all PBAs show this bidirectional behaviour while in practice, this behaviour has been reported for PBAs completely made of the same material and it is not established whether this behaviour happens

for PBAs whose layers are made of different materials.

Looking at the equations of the model, it can be noticed that the bending stiffness of the beam equals $E_b I_b = E_b \frac{b' h^3}{12} + 2E_m \left[\frac{b'-b}{12} e^3 + e \frac{b'-b}{2} \left(\frac{e+h}{2} \right)^2 \right]$. Hence, according to the numerical model, since the thicknesses h and e of the beam and the membrane are to the power three, they will have more influence on the PBA displacements than the widths b and b' of the cavity and the actuator, and than the Young's moduli E_b and E_m of the beam and the membrane.

If a dimensional analysis is performed on the model parameters (b' is not considered here) $L, b, E_m, E_b, e, h, p, \Delta x$ and Δy , the corresponding dimensionless numbers are $\pi_1 = \frac{e}{h}$, $\pi_2 = \frac{b}{h}$, $\pi_3 = \frac{L}{h}$, $\pi_4 = \frac{\Delta x}{h}$, $\pi_4' = \frac{\Delta y}{h}$, $\pi_5 = \frac{E_m}{E_b}$ and $\pi_6 = \frac{p}{E_b}$, which are linked by the following two relationships:

$$\pi_4 = \frac{\Delta x}{h} = f(\pi_1, \pi_2, \pi_3, \pi_5, \pi_6) \quad (6.38)$$

$$\pi_4' = \frac{\Delta y}{h} = g(\pi_1, \pi_2, \pi_3, \pi_5, \pi_6) \quad (6.39)$$

Hence, if the dimensionless numbers $\pi_1, \pi_2, \pi_3, \pi_5$ and π_6 keep the same values, $\pi_4 = \frac{\Delta x}{h}$ and $\pi_4' = \frac{\Delta y}{h}$ also keep the same values. This means that if the dimensions of the PBA L, b, e and h are multiplied by a given factor, the displacements Δx and Δy will increase by the same factor. Besides, if the Young's moduli E_m and E_b and the pressure p are multiplied by a given factor, the displacements Δx and Δy will not change.

The numerical model could be modified in order to predict the displacements of the actuator tip rather than the displacements of the cavity tip. This would allow a better comparison between the predictions of the numerical model and the measurements performed on Konishi's PBA and the test bench PBA.

However, at this stage, it is not possible to conclude whether the numerical model could be used to predict the qualitative effects, on the tip displacements, of the change of a PBA parameter. To answer this question, more experimental validations are required with prototypes whose parameters are perfectly known.